Molecular Biology of the Cell
Vol. 21, 470–480, February 1, 2010

A Cdc42 Activation Cycle Coordinated by PI 3-Kinase during Fc Receptor-mediated Phagocytosis

Peter Beemiller,*† Youxin Zhang,†‡ Suresh Mohan,§ Erik Levinsohn,§ Isabella Gaeta,§ Adam D. Hoppe,§‖ and Joel A. Swanson*‡§

*Cellular and Molecular Biology Graduate Program, and ‡Biophysics Graduate Program, University of Michigan, Ann Arbor, MI 48109-1055; §Department of Microbiology and Immunology, University of Michigan Medical School, Ann Arbor, MI 48109-5620; and ‖Department of Chemistry and Biochemistry, South Dakota State University, Brookings, SD 57007-0896

Submitted May 19, 2008; Revised November 9, 2009; Accepted November 19, 2009
Monitoring Editor: Yu-Li Wang

Fcγ Receptor (FcR)-mediated phagocytosis by macrophages requires phosphatidylinositol 3-kinase (PI3K) and activation of the Rho-family GTPases Cdc42 and Rac1. Cdc42 is activated at the advancing edge of the phagocytic cup, where actin is concentrated, and is deactivated at the base of the cup. The timing of 3′ phosphoinositide (3′PI) concentration changes in cup membranes suggests a role for 3′PIs in deactivation of Cdc42. This study examined the relationships between PI3K and the patterns of Rho-family GTPase signaling during phagosome formation. Inhibition of PI3K resulted in persistently active Cdc42 and Rac1, but not Rac2, in stalled phagocytic cups. Patterns of 3′PIs and Rho-family GTPase activities during phagocytosis of 5- and 2-μm-diameter microspheres indicated similar underlying mechanisms despite particle size–dependent sensitivities to PI3K inhibition. Expression of constitutively active Cdc42(G12V) increased 3′PI concentrations in plasma membranes and small phagosomes, indicating a role for Cdc42 in PI3K activation. Cdc42(G12V) inhibited phagocytosis at a later stage than inhibition by dominant negative Cdc42(N17). Together, these studies identified a Cdc42 activation cycle organized by PI3K, in which FcR-activated Cdc42 stimulates PI3K and actin polymerization, and the subsequent increase of 3′PIs in cup membranes inactivates Cdc42 to allow actin recycling necessary for phagosome formation.

INTRODUCTION

Fcγ receptor (FcR)-mediated phagocytosis occurs through a series of morphological stages, beginning when FcR on the surface of a phagocyte bind to IgG-class immunoglobulins that have coated (opsonized) particles. In conjunction with membrane remodeling at sites of phagocytosis, transient assembly of actin filaments pushes the macrophage plasma membrane over target particles (Swanson, 2008). This is followed by fusion of intracellular membranous compartments with the phagosome (Bajno *et al.*, 2000; Niedergang *et al.*, 2003) and myosin-dependent contractile activities that constrict the distal margins of the cup, closing the phagosome (Swanson *et al.*, 1999). During phagocytosis, actin depolymerization can occur at the base of the cup even as actin filaments continue to extend at the distal margin (Hoppe and Swanson, 2004). A central question regarding phagocytosis is how the ligation of a single kind of receptor, FcR, can generate this spatially organized sequence of distinct activities.

Type 1 phosphatidylinositol 3-kinase (PI3K) generates phosphatidylinositol (3,4,5)-trisphosphate [PI(3,4,5)P_3] and PI(3,4)P_2, and fluorescent reporters of 3′ phosphoinositide (3′PI) distributions in living cells indicate that 3′PIs are generated on the inner membranes of forming phagocytic cups (Botelho *et al.*, 2000; Marshall *et al.*, 2001; Vieira *et al.*, 2001). The PI3K inhibitors wortmannin and LY294002 block the activities required to complete phagocytosis of particles larger than 3 μm in diameter (Araki *et al.*, 1996; Cox *et al.*, 1999). In the presence of PI3K inhibitors, incomplete phagosomes persist as actin-rich phagocytic cups. This suggests that the 3′PIs generated by PI3K in phagosomal membranes organize later stages of phagocytosis which are required to complete internalization of large particles. It remains undetermined whether phagocytosis of large particles occurs by different mechanisms than small particles or if instead PI3K-dependent processes are present in both but only limiting for large particles.

FcR-mediated phagocytosis requires the Rho-family GTPases Cdc42 and Rac1 (Cox *et al.*, 1997; Caron and Hall, 1998), which regulate actin filament assembly and disassembly, and the ARF-family GTPases ARF1 and ARF6 (Zhang *et al.*, 1998; Beemiller *et al.*, 2006), which regulate membrane trafficking and remodeling (Honda *et al.*, 1999; Ge *et al.*, 2001; Melendez *et al.*, 2001; O'Luanaigh *et al.*, 2002). The GTPases alternate between inactive GDP-bound states and active GTP-bound states. GTP binding and activation are stimu-

This article was published online ahead of print in *MBC in Press* (http://www.molbiolcell.org/cgi/doi/10.1091/mbc.E08–05–0494) on December 2, 2009.

† Co-first author.

Address correspondence to: Joel A. Swanson (jswan@umich.edu).

Abbreviations used: CBD, Cdc42-binding domain; CFP, cyan fluorescent protein; FcR, Fcγ receptor; FRET, fluorescence resonance energy transfer; GAP, GTPase-accelerating protein; GEF, guanine nucleotide exchange factor; IgG, immunoglobulin G; PBD, p21-binding domain; 3′PI, 3′ phosphoinositide; PI3K, phosphatidylinositol 3-kinase; PI(3,4,5)P_3, phosphatidylinositol (3,4,5)-trisphosphate; PI(3,4)P_2, phosphatidylinositol (3,4)-bisphosphate; RFP, red fluorescent protein; YFP, yellow fluorescent protein.

© 2010 by The American Society for Cell Biology

lated by guanine nucleotide exchange factors (GEFs), whereas inactivation by GTP hydrolysis is accelerated by GTPase-activating proteins (GAPs). The active GTPases regulate distinct combinations of effector kinases and downstream activities, including actin polymerization and depolymerization, myosin contractility, and vesicle fusion with plasma membranes.

Studies of phagocytosis in macrophages expressing fluorescent chimeras indicate three patterns of GTPase activity during FcR-mediated phagocytosis (Hoppe and Swanson, 2004; Beemiller *et al.*, 2006). Although ratiometric fluorescence microscopy showed that Cdc42, Rac1, and Rac2 are present on phagosomal membranes throughout phagosome formation (Figure 2 of Hoppe and Swanson, 2004), fluorescence resonance energy transfer (FRET)-based stoichiometric methods (Hoppe *et al.*, 2002) revealed distinct patterns of activation and deactivation. Cdc42, Rac1, and ARF6 are active (i.e., GTP-bound) at the advancing edge of phagocytic cups. Cdc42 and ARF6 become inactive a short distance from the distal margin of the phagocytic cup, but Rac1 remains active throughout phagosome formation and is inactivated only upon phagosome closure. Rac2 and ARF1 activation are delayed and localized to the base of the phagocytic cup, where they remain activated until after phagosome closure. Actin is often concentrated at the advancing edge of the phagocytic cup, similar to the distributions of active Cdc42 and ARF6.

Some of the GEFs and GAPs that control GTPase activities during phagocytosis may be regulated by 3′PIs. Many GEFs and GAPs contain pleckstrin-homology (PH) domains, which tether the proteins to 3′PIs in membranes and are necessary for their activities. Consistent with this model, ARF1 and ARF6 are coordinately regulated by PI3K in response to FcR ligation. Inhibition of PI3K with LY294002 blocked the activation of ARF1 and deactivation of ARF6, such that unclosed phagocytic cups contained persistently activated ARF6 and basal levels of activated ARF1 (Beemiller *et al.*, 2006). This indicated that PI3K mediates a signal transition in which the generation of 3′PIs on phagocytic membranes activates the GAPs that deactivate ARF6 and the GEFs that activate ARF1. If a localized increase in 3′PIs is a general mechanism coordinating the movements of phagocytosis, then the Rho-family GTPases should also exhibit a signal transition. Accordingly, in the phagocytic cups of LY294002-inhibited macrophages, Cdc42 should be persistently activated and Rac2 should remain inactive. As the patterns of Rac1 activity in phagocytosis differ from ARF1 and ARF6, it is not clear how its activation would respond to PI3K inhibition.

This study used quantitative fluorescence microscopy to examine the regulation of PI3K, actin and Rho-family GTPases during FcR-mediated phagocytosis. These methods allowed comparisons of signal timing and distribution during phagocytosis of erythrocytes and of large and small microspheres. We show that the PI3K-dependent signal transition is required for phagocytosis. Specifically, interdependent activities of PI3K and the Cdc42 activation cycle organize actin dynamics in the phagocytic cup.

MATERIALS AND METHODS

Tissue Culture, Transfection, and PI3K Inhibition

RAW264.7 cells from the American Type Culture Collection (Manassas, VA) were cultured in Advanced DMEM supplemented with 2% heat-inactivated FBS, 4 mM L-glutamine, 20 U/ml penicillin, and 20 μg/ml streptomycin. All cell culture products were purchased from Invitrogen (Carlsbad, CA). To prepare cells for time-lapse fluorescence microscopy, $\sim 2.5 \times 10^5$ cells were plated onto acid-washed 25-mm coverslips 18–24 h before imaging. For phagocytosis assays, $\sim 5 \times 10^4$ cells were plated onto 12-mm coverslips.

Constructs for yellow fluorescent protein (YFP)-AktPH domain, YFP-Cdc42/Rac, and cyan fluorescent protein (CFP)-PBD constructs were described previously (Hoppe and Swanson, 2004). YFP-CBD was constructed by inserting the Cdc42-binding domain (CBD) from WASP into the YFP vector at XhoI/EcoRI sites (gift from Matthew Krummel, UCSF). Cells were transfected using FuGene-6 or Fugene-HD (Roche Diagnostics, Indianapolis, IN). For time-lapse FRET imaging, $\sim$1 μg of plasmid DNA for YFP-Cdc42, YFP-Rac, or PBD-CFP was used for each coverslip, and 1.2 μg YFP-CBD and 0.8 μg CFP or 0.8 μg YFP-Cdc42(G12V), 1 μg mCFP-AktPH, and 0.4 μg mCherry was used for each coverslip for time-lapse ratiometric imaging. Transfection for phagocytosis assays was accomplished using $\sim$300 ng DNA for YFP, YFP-Cdc42, or YFP-Rac. The plasmids described here are available through Addgene (www.addgene.com/Joel_Swanson). To test for PI3K inhibition, macrophages were pretreated with 50 μM LY294002 or 100 nM TGX-221 (EMD Chemicals, Gibbstown, NJ) for 30 min in complete medium. Opsonized microspheres were then added, and phagocytosis efficiency was assessed.

Microsphere Opsonization

Streptavidin-coated, silica microspheres of 2- and 5-μm diameters were purchased from Corpuscular (Cold Spring Harbor, NY) and Bangs Laboratories (Fisher, IN), respectively. To prepare beads with equivalent surface concentrations of IgG, aliquots of 2- and 5-μm beads representing an equal surface area (corresponding to 50–100 μg of 5-μm microspheres) were resuspended in phosphate-buffered saline (PBS) plus 1% bovine serum albumin (BSA) and incubated at room temperature with various concentrations of anti-streptavidin polyclonal IgG (Abcam, Cambridge, MA). After opsonization, beads were rinsed three times with PBS-BSA to remove unbound IgG. Beads were resuspended in SDS-PAGE loading buffer and heated to 95°C for 5 min to elute the bound IgG. The eluted IgG was Western blotted to estimate the amount of IgG on the particles (Supplemental Figure S1). Each lot of microspheres was tested to ensure equivalent opsonization. IgG-opsonized sheep erythrocytes were prepared as described previously (Knapp and Swanson, 1990).

Phagocytosis Efficiency Assays

RAW264.7 cells were transfected with plasmids for YFP, YFP fusions to wild-type Cdc42 or Rac, or YFP fusions to constitutively active mutants of Cdc42 or Rac. After $\sim$18 h, opsonized 2- and 5-μm microspheres were added, and the macrophages were allowed to internalize the particles for 30 min at 37°C. *Cells were then rinsed with PBS, fixed in 4% paraformaldehyde for 30 min at room temperature, and rinsed again, and the nonspecific binding sites were blocked with PBS plus 2% goat serum. After rinsing with PBS, beads that were not completely internalized were marked with Alexa 595–conjugated goat anti-rabbit IgG (Invitrogen). Phagocytic efficiencies (the percent of bound particles successfully internalized by macrophages) were counted for at least 25 macrophages per coverslip. Phagocytic efficiencies in cells expressing fusion proteins were divided by the phagocytic efficiencies in macrophages expressing YFP (typically $\sim$60–75%). Statistical analysis was performed on data from at least two experiments in Prism 3 (GraphPad Software, San Diego, CA).

FRET Microscopy, Ratiometric Microscopy, and Image Processing

Component FRET images (I_A, I_D, and I_F representing YFP acceptor, CFP donor, and FRET images, respectively), ratiometric images (I_A and I_D) and phase-contrast images were acquired on an inverted Eclipse TE-300 microscope (Nikon USA, Melville, NY) through a 60×, 1.4 NA, oil-immersion objective (Nikon USA). Epifluorescence illumination was provided by a Lambda LS Xenon arc lamp (Sutter Instrument Company, Novato, CA). Transmitted light illumination was controlled by a Uniblitz VMM-D1 shutter driver (Vincent Associates, Rochester, NY). A JP4v2 CFP/YFP filter set (Chroma Technology, Rockingham, VT) controlled by a Lambda 10-2 filter wheel controller (Sutter Instrument Company) was used to select wavelengths for CFP, YFP, and FRET image acquisition. Images were recorded with a CoolSnap HQ cooled-CCD camera (Roper Scientific, Tucson, AZ). All hardware was controlled using Metamorph 6.1 or 6.2 (Molecular Devices, Downingtown, PA). Calculation of the FRET stoichiometry images E_A, the fraction of *acceptor* molecules in complex with donor molecules times the efficiency of energy transfer, E_D, the fraction of *donor* molecules in complex with acceptor molecules times the efficiency of energy transfer, and R_M, the molar ratio of acceptors to donors, corrected for suppression of donor fluorescence by energy transfer, were performed in Metamorph using the shade/bias corrected images as described previously (Beemiller *et al.*, 2006). To convert E_A values to G* values, which represent the fraction of YFP-GTPases in the GTP-bound state, the mean cellular ratio of acceptors to donors and the characteristic FRET efficiency of the YFP-GTPase:CFP-PBD complexes were used as described previously (Hoppe and Swanson, 2004).

Recruitment indexes (R_i), which represent the cell volume– and transfection efficiency–normalized translocation of probes to the phagosome region, were

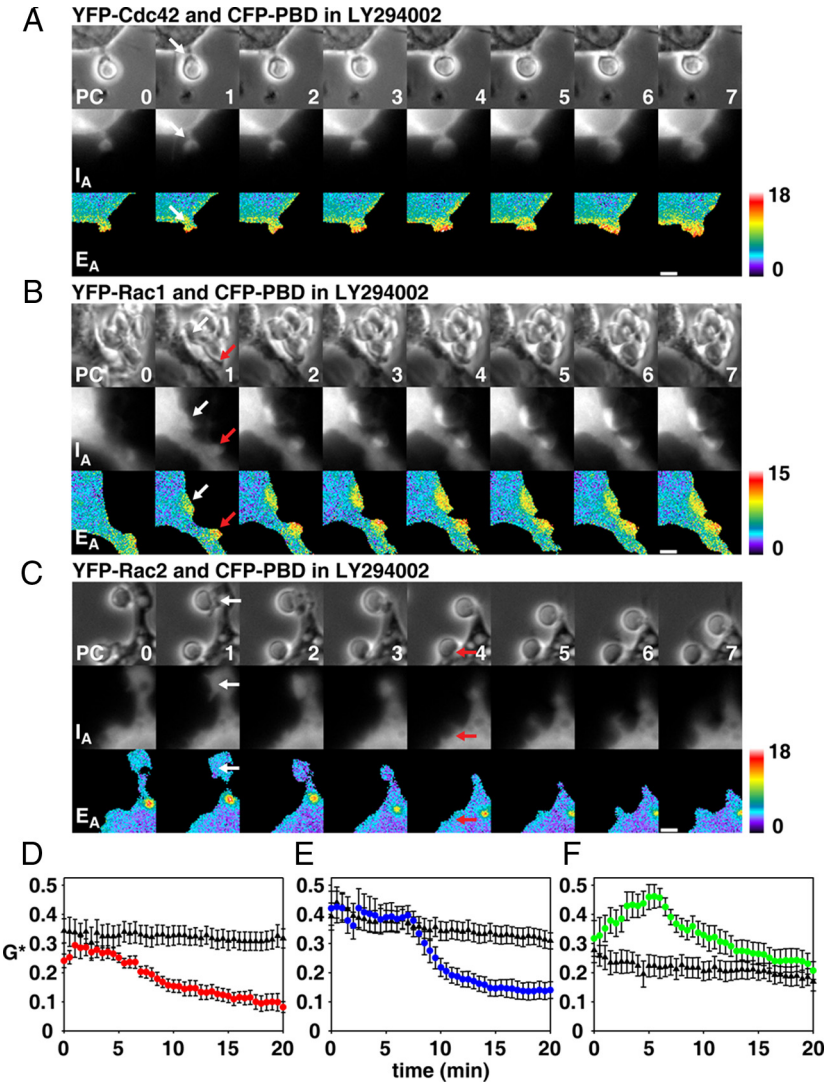

Figure 1. Activation of Rho GTPases in phagocytic cups after LY294002 inhibition. Activation of YFP-Cdc42 (A), YFP-Rac1 (B) and YFP-Rac2 (C) was measured by FRET microscopy in LY294002-treated macrophages during phagocytic cup formation around IgG-opsonized erythrocytes. (A–C) The image series show phase-contrast (PC), YFP-Cdc42/Rac (I_A), and pseudocolored E_A images indicating GTPase activation. White and red arrows indicate phagocytic cups. Scale bars at bottom right, 3 μm. Numbers in the bottom right of the PC images indicate the time in minutes after binding of the first erythrocyte. E_A values of pseudocolor images in A–C correspond to G* values of 0.74, 0.68, and 0.97, respectively. (D–F) GTPase activation in LY294002-treated macrophages (▲) was quantified and compared with activation by control macrophages (colored circles) (D) Cdc42, (E) Rac1, (F) Rac2. For each plot, n = 10–13 sequences. Error bars, (D–F) ±SEM.

calculated as described previously (Hoppe and Swanson, 2004). In cells expressing constitutively active Cdc42, R_i was obtained from the ratio image between the CFP and red fluorescent protein (RFP; mCherry) channels. In control cells, R_i was obtained from the ratio images of the YFP and CFP channels.

To measure FRET or R_i as a function of time during phagocytosis, the TRACKOBJ particle-tracking algorithm of Metamorph was used to identify and track erythrocytes or microspheres bound by macrophages and to automate the measurement of average gray values in a predefined measurement circle centered around the target particle, as described previously (Henry *et al.*, 2004; Hoppe and Swanson, 2004). A 2.2-μm-diameter circle was used for 2-μm microspheres, and a 5.4-μm circle was used for erythrocytes and 5-μm microspheres. Particle traces for independent phagocytic events were aligned using the frame of each YFP image series in which a phagocytic cup was first detectable.

We learned in these studies that erythrocytes and 5-μm microspheres did not behave identically, despite their similar size and geometry. The rigidity of the microspheres prevented cells from forming stable half-cups after inhibitor treatments. This appeared to result from contractile activities of phagocytosis, which squeezed cups formed around more deformable erythrocytes, consequently stabilizing them as stalled half-cups, but which caused partially formed cups around large, rigid microspheres to retract. This did not affect overall phagocytic indexes, but it complicated measurements of FRET signals from half-cups around microspheres. Therefore, experiments that quantified signals in half-formed cups were performed using IgG-opsonized erythrocytes (see Figures 1, 2, and 6), whereas those that compared phagocytic index and signals between large and small particles were performed using IgG-opsonized microspheres (see Figures 3–5).

To measure relative recruitment of CFP-AktPH to membranes in resting cells, line scans were performed in two lines perpendicular to each other in ratio images. Three pixels with nonzero values on each end of the line were picked as the membrane region, and pixels between them were defined as the cytosol region. Average values from the membrane region were divided by average values from the cytosol region on the two perpendicular lines to generate relative recruitment to membrane (Rm/Rc). As for Ri, this relative recruitment to membrane was normalized for cell volume and transfection efficiency.

RESULTS

Rho-Family GTPases Are Coordinately Regulated by PI3K during Phagocytosis

Prompted by the similarities between the activation profiles of ARF- and Rho-family GTPases (Hoppe and Swanson, 2004; Beemiller *et al.*, 2006), we used FRET microscopy to determine which Rho-family GTPases were activated in phagocytic cups of macrophages in LY294002. GTPase activities at sites of phagocytosis were measured by applying FRET stoichiometry (Hoppe *et al.*, 2002; Beemiller *et al.*, 2006) to images of cells expressing CFP-labeled p21-binding domain (CFP-PBD) and either YFP-Cdc42, YFP-Rac1, or YFP-Rac2. PBD is the Cdc42/Rac-binding domain from p21-activated kinase-1 (PAK1), which binds specifically to Cdc42 or Rac GTPases in their GTP-bound conformations (Manser *et al.*, 1993). Component fluorescence images of macrophages performing phagocytosis of IgG-opsonized sheep erythrocytes were collected at 30-s intervals and E_A images,

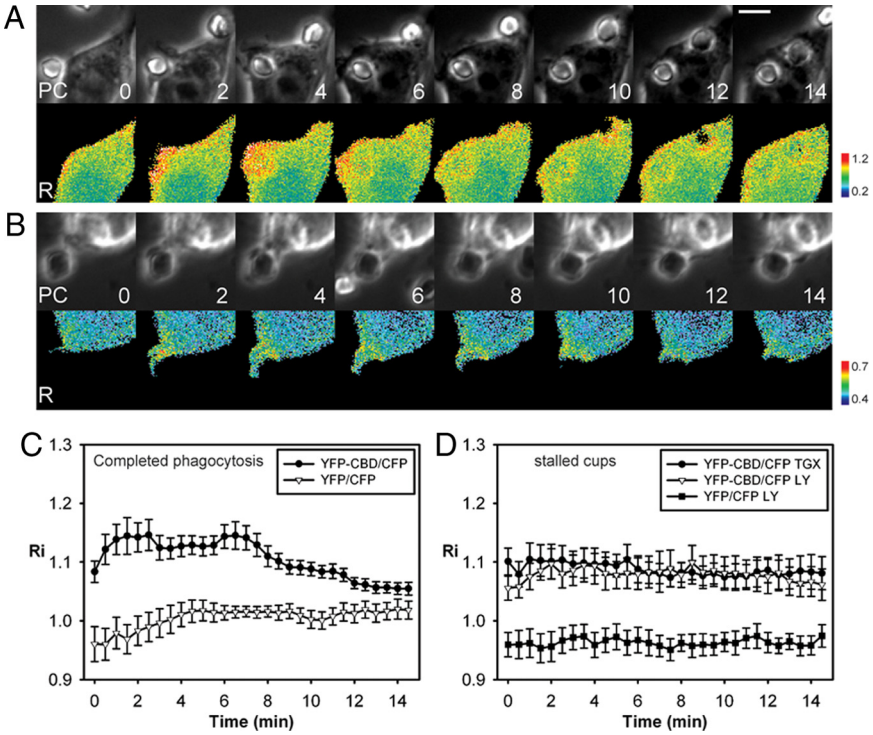

Figure 2. Activation of endogenous Cdc42 during phagocytosis. (A and B) Phase-contrast (top) and ratio images (bottom) of RAW264.7 macrophages expressing YFP-CBD and CFP show that endogenous Cdc42 was activated at the leading edge of phagocytic cups during complete phagocytosis (A) and remained activated on incomplete cups formed by TGX-221-treated macrophages (B). Scale bar, 5 μm. (C) Recruitment index of YFP-CBD (●) and free YFP (▽), as a negative control, show that endogenous Cdc42 was activated on phagosomes early during phagocytosis and deactivated after internalization was complete, (n = 11). (D) Recruitment indexes of YFP-CBD on incomplete phagocytic cups formed by TGX-221-treated (●) and LY294002-treated (△) macrophages were higher than that of free YFP on incomplete phagocytic cups formed by LY294002-treated macrophages (■), indicating that PI(3,4,5)P_3 regulates the deactivation of endogenous Cdc42, n = 8. Error bars, ±SEM.

which indicate the fraction of YFP-GTPase bound to CFP-PBD, were calculated as described previously (Hoppe *et al.*, 2002; Beemiller *et al.*, 2006). These experiments were performed using IgG-opsonized erythrocytes, so that the results could be compared with previous studies of ARF1 and ARF6 in phagocytosis (Beemiller *et al.*, 2006). RAW264.7 macrophages expressing YFP-Cdc42 and CFP-PBD and pretreated with LY294002 showed activated Cdc42 immediately after particle binding (Figure 1A). However, in contrast to control phagosomes, Cdc42 remained activated in the persistent, unclosed cups (observation period ~20 min). The magnitude of activation, measured as the fraction of YFP-Cdc42 in the GTP-bound state (G*; see Hoppe and Swanson, 2004) was similar to the peak level of activation in control macrophages (Figure 1D).

This analysis was repeated using YFP-Rac1. Rac1 activation is PI3K-dependent in some cells (Srinivasan *et al.*, 2003). However, macrophages in LY294002 showed rapid activation of Rac1 in response to bound opsonized erythrocytes (Figure 1B). Like Cdc42 and ARF6 (Beemiller *et al.*, 2006), Rac1 activation persisted in the unclosed phagocytic cups. LY294002 treatment did not delay Rac1 activation or decrease the magnitude of Rac1 activation (Figure 1E), indicating that Rac1 activation was PI3K-independent.

In contrast, the FRET microscopy indicated little activation of YFP-Rac2 in the unclosed phagocytic cups (Figure 1C). Unlike control phagocytic events, which displayed a prominent spike in activation during phagosome closure, the persistent, unclosed cups of LY294002-treated macrophages showed basal levels of activated Rac2 (Figure 1F). Thus, Cdc42, Rac1, and Rac2 showed strikingly different activation properties after inhibition of PI3K: Cdc42 and Rac1 were persistently active in cups, whereas Rac2 remained inactive.

Deactivation of Endogenous Cdc42 Is Regulated by PI3K during Phagocytosis

To confirm that activities of endogenous Cdc42 are also regulated by PI3K, the localization of YFP-labeled Cdc42-binding domain from WASP (YFP-CBD), which binds to GTP-Cdc42 (Cannon *et al.*, 2001; Tskvitaria-Fuller *et al.*, 2006), was measured by ratiometric fluorescence microscopy during phagocytosis. The recruitment index, a cell volume– and transfection efficiency–normalized indicator of YFP-chimera recruitment to phagosomes, was measured during phagocytosis of sheep erythrocytes. Consistent with the FRET microscopy, YFP-CBD was recruited early during phagocytosis (Figure 2A). The recruitment was highest at the leading edge of phagocytic cups. The recruitment of YFP-CBD to the base of the cups decreased less than the decrease observed by FRET microscopy (Hoppe and Swanson, 2004), possibly due to different Cdc42-binding properties of CBD and PBD. Because the YFP-CBD recruitment produced a low R_i signal (Figure 2C), recruitment was compared with similar phagocytosis events using YFP as a negative control (Figure 2C). The difference between the Ri of YFP-CBD and YFP represented the magnitude of YFP-CBD recruitment during phagocytosis. YFP-CBD was recruited to phagosomes immediately after phagocytosis began and continued until internalization was completed (Figure 2C), confirming that the activities of endogenous Cdc42 during phagocytosis were similar to the activities measured by FRET stoichiometry.

YFP-CBD was also recruited to stalled phagocytic cups formed in LY294002-treated macrophages and remained in the cups, indicating persistent activation of endogenous Cdc42 (Figure 2D). Because LY294002 inhibits both type I and type III PI3K, we also measured endogenous Cdc42 activities using another PI3K inhibitor, TGX-221, which is specific for the β- and δ-isoforms of type I PI3K (Chaussade *et al.*, 2007). YFP-CBD was also recruited to unfinished cups formed in TGX-221–treated cells (Figure 2, B and D) and persisted in those cups, suggesting that Cdc42 deactivation required the type I PI3K products PI(3,4,5)P_3 and PI(3,4)P_2.

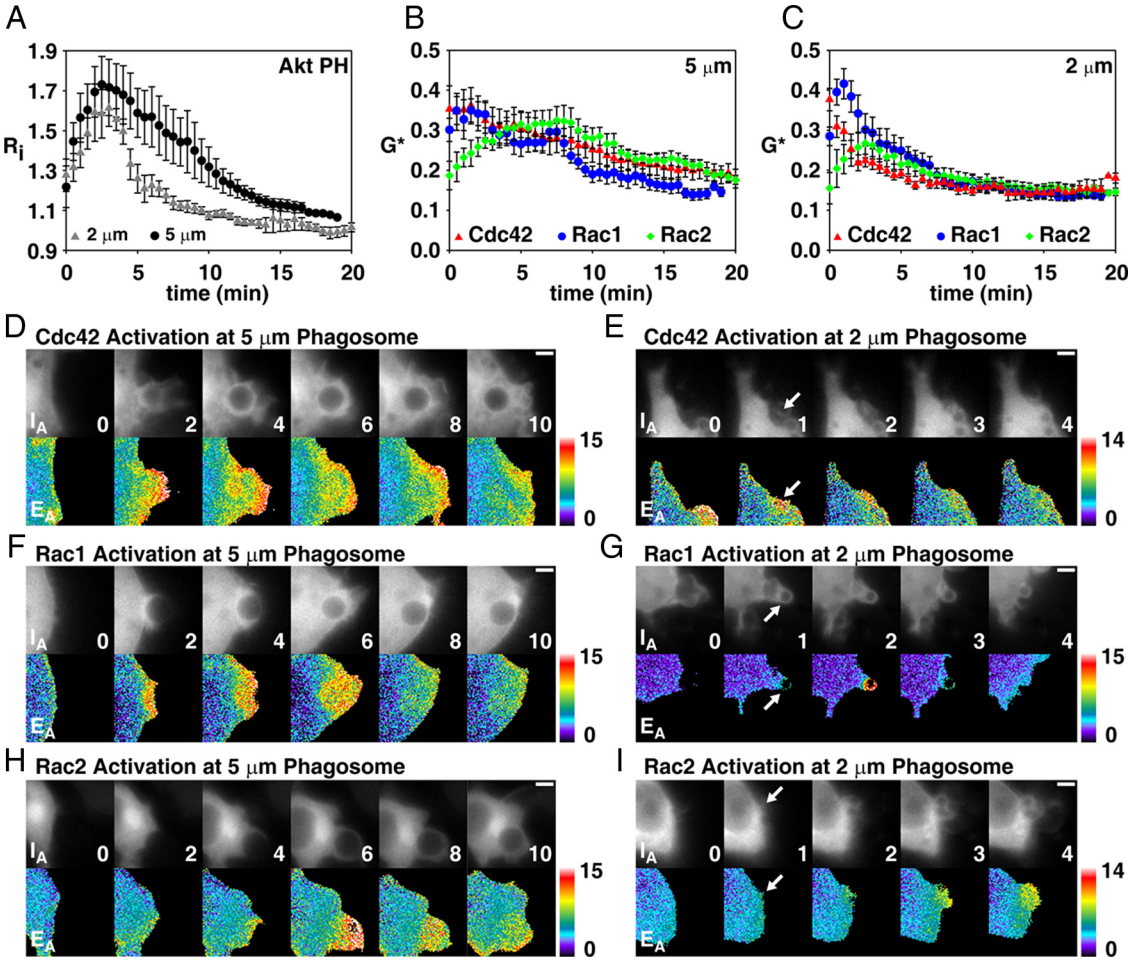

Figure 3. The signal transition is present during phagocytosis of small and large particles. (A) 3′PI dynamics on phagosomes were measured using ratiometric imaging of YFP-AktPH; 2-μm phagosomes (gray triangles): n = 7; 5-μm phagosomes (●): n = 5. (B and C) G* indicates the fraction of YFP-Cdc42, YFP-Rac1, or YFP-Rac2 activated in each pixel during phagocytosis of 2- and 5-μm diameter microspheres. (B) Cdc42, Rac1, and Rac2 activation during phagocytosis of 5-μm microspheres; n = 9, 9, and 8 phagocytic events for Cdc42, Rac1, and Rac2, respectively. (C) Activation of Cdc42, Rac1, and Rac2 during phagocytosis of 2-μm microspheres; n = 12, 11, and 13 phagocytic events for Cdc42, Rac1, and Rac2, respectively. (D, F, and H) I_A and E_A image series are presented for uptake of 5-μm microspheres by macrophages expressing CFP-PBD and either YFP-Cdc42 (D), YFP-Rac1 (F), or YFP-Rac2 (H). (E, G, and I) I_A and E_A image series showing activation of Cdc42 (E), Rac1 (G), or Rac2 (I) during phagocytosis of 2-μm particles. White arrows indicate microspheres undergoing phagocytosis. Numbers at the bottom right of I_A images represent the time (min) after the first appearance of the phagocytic cup. Scale bars, (D–I) 3 μm.

Large and Small Particles Stimulate Similar Signaling Patterns during Phagocytosis

PI3K inhibitors have less effect on phagocytosis of 2-μm diameter particles than 5-μm particles (Cox *et al.*, 1999). The differential sensitivity of small and large particle phagocytosis to PI3K inhibition suggests that different signals regulate phagocytosis of small and large particles. We therefore examined whether differences in 3′PI synthesis or GTPase activation patterns during phagocytosis of different sizes of particles could explain the size-dependence of inhibition by PI3K inhibitors. Streptavidin-coated silica microspheres of 2- and 5-μm diameter were opsonized with equivalent levels of IgG-labeling per unit surface area (see *Materials and Methods* and Supplemental Figure S1). To compare the 3′PI responses during phagocytosis, macrophages expressing CFP and a YFP fusion to the PH domain of Akt (YFP-AktPH) were presented opsonized 2- and 5-μm microspheres and observed by ratiometric fluorescence imaging. AktPH binds to PI(3,4,5)P_3 and PI(3,4)P_2 (Kavran *et al.*, 1998). Subcellular localization of fluorescent AktPH chimeras has been used previously to localize activity of PI3K (Vieira *et al.*, 2001; Hoppe and Swanson, 2004). Quantitative measures of multiple phagocytic events showed that, for both 2- and 5-μm phagosomes, the maximum 3′PI accumulation appeared ~2–3 min after the initiation of pseudopod extension (Figure 3A). Thus, phagocytosis of both small and large particles generated robust, localized 3′PI responses of similar magnitudes.

We then measured the activation dynamics of the Rho GTPases during phagocytosis of small and large microspheres. Cdc42 was activated during phagocytosis of both 2 μm and 5-μm microspheres, with peak activation of Cdc42 occurring within the first few minutes of pseudopod extension (Figure 3, B–E). Cdc42 activation per unit area in the distal margins of phagosomes was essentially identical on 2- and 5-μm phagosomes (compare initial time points in Figures 3, B and C). Rac1 activity was slightly delayed relative to Cdc42 on 2-μm phagosomes (Figure 3C). YFP-Rac2 was activated gradually during formation of 5-μm phagosomes (Figure 3, B and H). Peak levels were reached later than the

peaks in YFP-AktPH recruitment (cf. Figure 3, A and B). Peak Rac2 activation levels were ~20% lower than those observed at 5-μm microsphere phagosomes (Figure 3, B and C). These patterns and magnitudes of activation indicated that the signal transition occurred during phagocytosis of both large and small beads. The peak of Cdc42 activation preceded the peak of PI(3,4,5)P_3 accumulation, which preceded the peak of Rac2 activation, whereas Rac1 activation spanned the signal transition.

Activation dynamics of Cdc42, Rac1, and Rac2 were also observed during complete phagocytosis of 2-μm microspheres by macrophages pretreated with LY294002. Cdc42 was not deactivated after phagosome closure, but remained active on phagosomes for at least 20 min (Supplemental Figure S2). In contrast, Rac1 deactivation followed closure of phagosomes. Rac2 was not activated on 2-μm microsphere phagosomes (Supplemental Figure S2), indicating that its activation was regulated by PI3K-generated 3′PIs, rather than by closure. Thus, the deactivation of Cdc42 and the activation of Rac2 correlated directly with 3′PI generation on phagosomal membranes.

Deactivation of Cdc42 Is Required to Complete Phagocytosis

We next investigated whether the PI3K-dependent deactivation of Cdc42 was required for phagocytosis of large or small particles. As macrophages likely express many potential GAPs for Cdc42 and Rac, and the identities of the GAPs required for phagocytosis are not known, we mimicked the loss of GAP activity by overexpressing constitutively active GTPase mutants. Phagocytic indexes were measured in macrophages overexpressing wild-type or constitutively active YFP-chimeras of Cdc42, Rac1, or Rac2. Constitutively active YFP-Rac1(Q61L) or YFP-Rac2(G12V) did not inhibit phagocytosis of 2- or 5-μm particles, suggesting that deactivation of Rac1 or Rac2 were not required for phagocytosis (Figure 4A). However, cells expressing YFP-Cdc42(G12V) showed a small reduction in the phagocytosis of 2-μm microspheres, and a significantly reduced uptake of 5-μm microspheres ($p < 0.001$). This indicated that deactivation of Cdc42 was necessary for closure of phagosomes, especially over large particles.

To examine whether phagocytosis of 2-μm microspheres is independent of the signal transition, phagocytic indexes of 2- or 5-μm particles were measured in cells expressing Cdc42(G12V) and exposed to LY294002. This double inhibition reduced the phagocytic indexes of 2- and 5-μm particles to about half of that seen under single inhibition (Figure 4B), indicating that phagocytosis of 2-μm microspheres also requires the signal transition. This further suggests that phagocytosis of 2-μm microspheres uses the same signals as phagocytosis of 5-μm microspheres, but that the PI3K-dependent late activities are not sufficiently inhibited by LY294002 to arrest phagocytosis. The fact that double inhibition by Cdc42(G12V) overexpression and LY294002 treatment led to lower phagocytic index than either inhibition alone indicated that Cdc42 deactivation and PI3K activation are parallel and additive activities.

Multiple Feedback Responses Stimulate PI3K

Previous biochemical studies found that Cdc42-GTP binds and activates PI3K (Zheng *et al.*, 1994; Usui *et al.*, 2003), but its role in regulating PI3K during FcR-mediated phagocytosis has not been examined. To study the effect of Cdc42 activation on PI3K, we monitored PI(3,4,5)P_3 generation by ratiometric imaging of macrophages coexpressing CFP-AktPH, mCherry, and mCit-Cdc42(G12V) and control cells

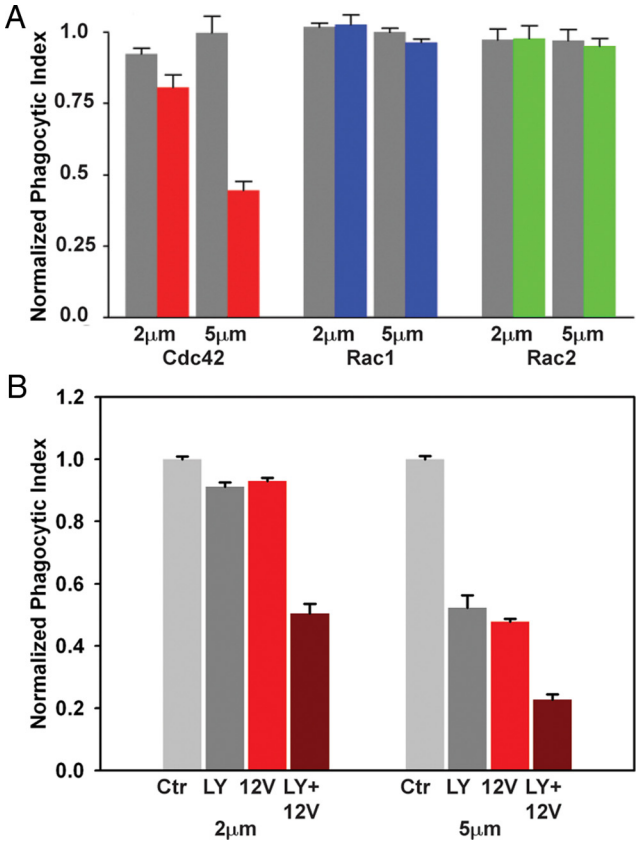

Figure 4. PI3K inhibition and constitutively active Cdc42 reduce phagocytosis additively. (A) Relative phagocytic indexes (the phagocytic efficiency of GTPase-transfected cells relative to control cells expressing YFP) of macrophages overexpressing YFP-Cdc42 (gray bars) or YFP-Cdc42(G12V) (red), YFP-Rac1(Q61L) (blue) and YFP-Rac2(G12V) (green) were measured for opsonized 2- and 5-μm microspheres. Cdc42(G12V) produced a particle size-dependent inhibition of phagocytosis. Active Rac mutants were not inhibitory. Error bars, ±SEM. (B) Phagocytic index of untransfected RAW 264.7 macrophages not treated (light gray) or treated (dark gray) with LY294002 and macrophages expressing YFP-Cdc42(G12V) not treated (red) or treated (dark red) with LY294002 were measured for 2- and 5-μm microspheres. All values were normalized to the phagocytic index of untransfected, untreated macrophages. Error bars, ±SEM.

expressing YFP-AktPH and CFP. In control cells, YFP-AktPH was uniformly distributed within the cell (Figure 5, A and C), indicating low PI(3,4,5)P_3 on cell membranes. In contrast, cells overexpressing YFP-Cdc42(G12V) showed CFP-AktPH recruitment to the membranes of resting cells, even before phagocytosis started (Figure 5, B and C), indicating that Cdc42(G12V) increased overall PI3K activity in resting macrophages.

To ask if active Cdc42 enhanced PI3K activity during phagocytosis, we measured CFP-AktPH recruitment during ingestion of 2-μm microspheres by macrophages expressing YFP-Cdc42(G12V). CFP-AktPH was recruited to phagosomes to a higher level and for a longer duration in macrophages overexpressing YFP-Cdc42(G12V) than in control cells (Figure 5, D and F–I), indicating that YFP-Cdc42(G12V) promoted PI3K activity to generate more PI(3,4,5)P_3 during successful phagocytosis. YFP-Cdc42(G12V) overexpression inhibited the closure of 5-μm phagosomes but not cup formation (Figure 5, L and M), allowing the measurement of

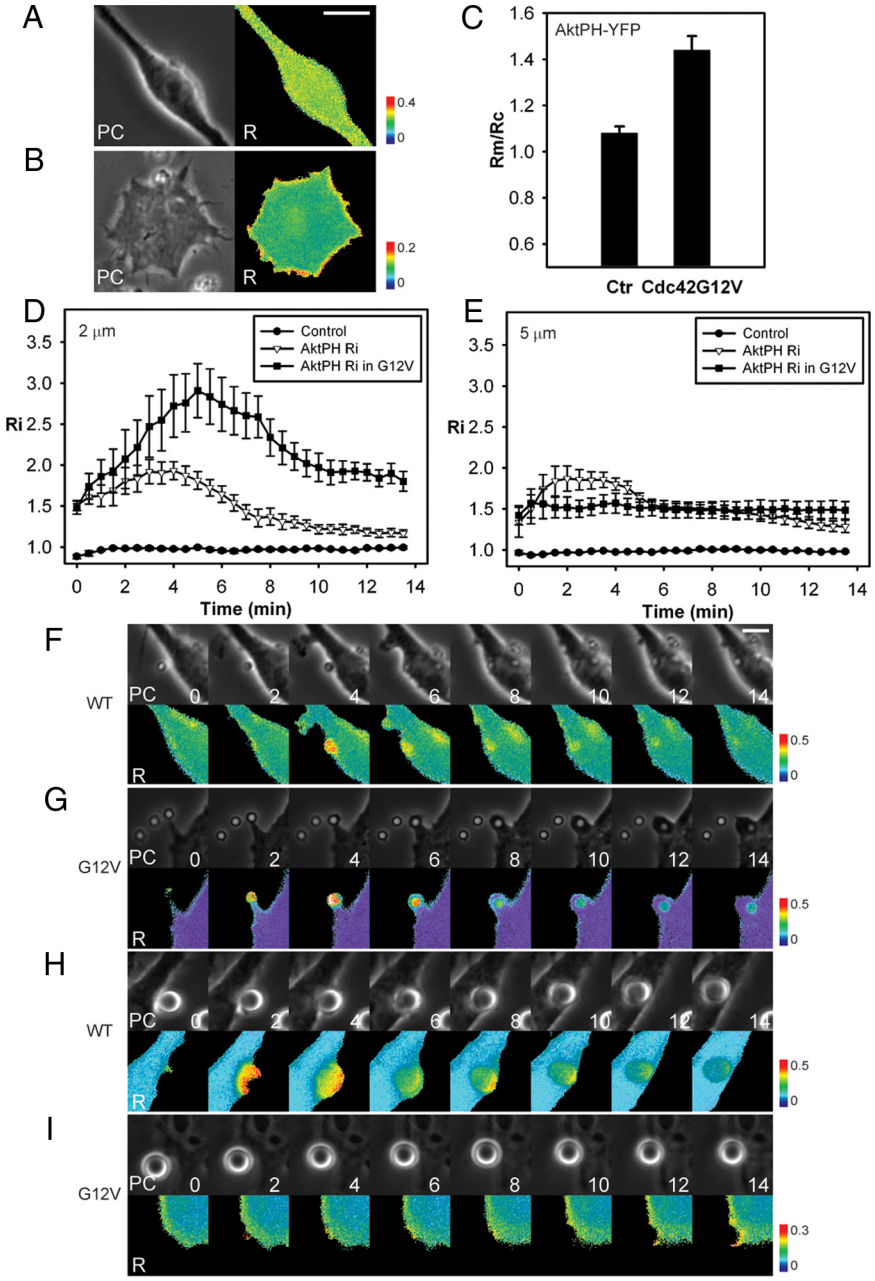

Figure 5. Cdc42(G12V) stimulates PI3K activity during phagocytosis. (A) Phase-contrast and ratio images of RAW264.7 macrophages expressing YFP-AktPH and CFP. PI(3,4,5)P_3 was not generated on membranes of resting cells. (B) Phase and ratio images of RAW264.7 macrophages expressing CFP-AktPH, YFP-Cdc42(G12V), and mCherry. PI(3,4,5)P_3 was generated on membranes of resting cells overexpressing Cdc42(G12V). (C) Relative CFP-AktPH recruitment to membranes (Rm/Rc) was measured in control cells and in cells expressing YFP-Cdc42(G12V); n = 6. (D and E) YFP recruitment (control) and CFP-AktPH recruitment to 2- (D) and 5-μm (E) phagosomes were measured by ratiometric imaging; n = 7. Error bars, ±SEM. Phase and ratio images of macrophages without (F and H) or with Cdc42(G12V) (G and I) during phagocytosis of 2- (F and G) and 5-μm (H and I) microspheres. Scale bars, 5 μm.

CFP-AktPH recruitment to the stalled phagocytic cups. CFP-AktPH was recruited to those stalled phagocytic cups, with a value significantly higher than baseline value (acquired from cells expressing free YFP and CFP; Figure 5E). This indicated that PI(3,4,5)P_3 generation is upstream of Cdc42 deactivation in signaling for phagocytosis. However, CFP-AktPH recruitment was less than that observed during complete phagocytosis in macrophages without Cdc42(G12V) overexpression (Figure 5, E, H, and I), indicating that although PI3K was stimulated by active Cdc42, a feedback from some late-stage signal or from some activity that follows phagosome closure was required for maximum PI3K activation.

Cdc42 Mutants Arrest Actin Dynamics at Different Stages of Phagosome Formation

The similar patterns of actin movement and of Cdc42 activity observed by FRET microscopy of phagocytic cups suggested that the Cdc42 activity cycle is necessary for actin movement during phagocytosis. Inhibition of phagocytosis by both dominant negative Cdc42(N17) (Cox *et al.*, 1997; Caron and Hall, 1998) and constitutively active Cdc42(G12V) suggests that the cycle of Cdc42 activation and deactivation effects proper actin dynamics. Accordingly, Cdc42(N17) should inhibit phagocytosis at an earlier stage than Cdc42(G12V). We therefore examined how Cdc42 governs the localization and dynamics of actin at forming phagosomes, using macrophages expressing mCherry-actin, CFP and YFP linked to either wild-type Cdc42, Cdc42(G12V), or Cdc42(N17) (Figure 6, A–C). In macrophages expressing wild-type Cdc42, phagocytosis was finished and mCherry-actin was recruited, starting at the base of the phagosome and moving toward the distal margin of the cup (Figure 6A). Actin extension to the distal margin of the phagosome was coupled with depolymerization of actin at the base of the cup. Macrophages expressing YFP-Cdc42(G12V) or YFP-

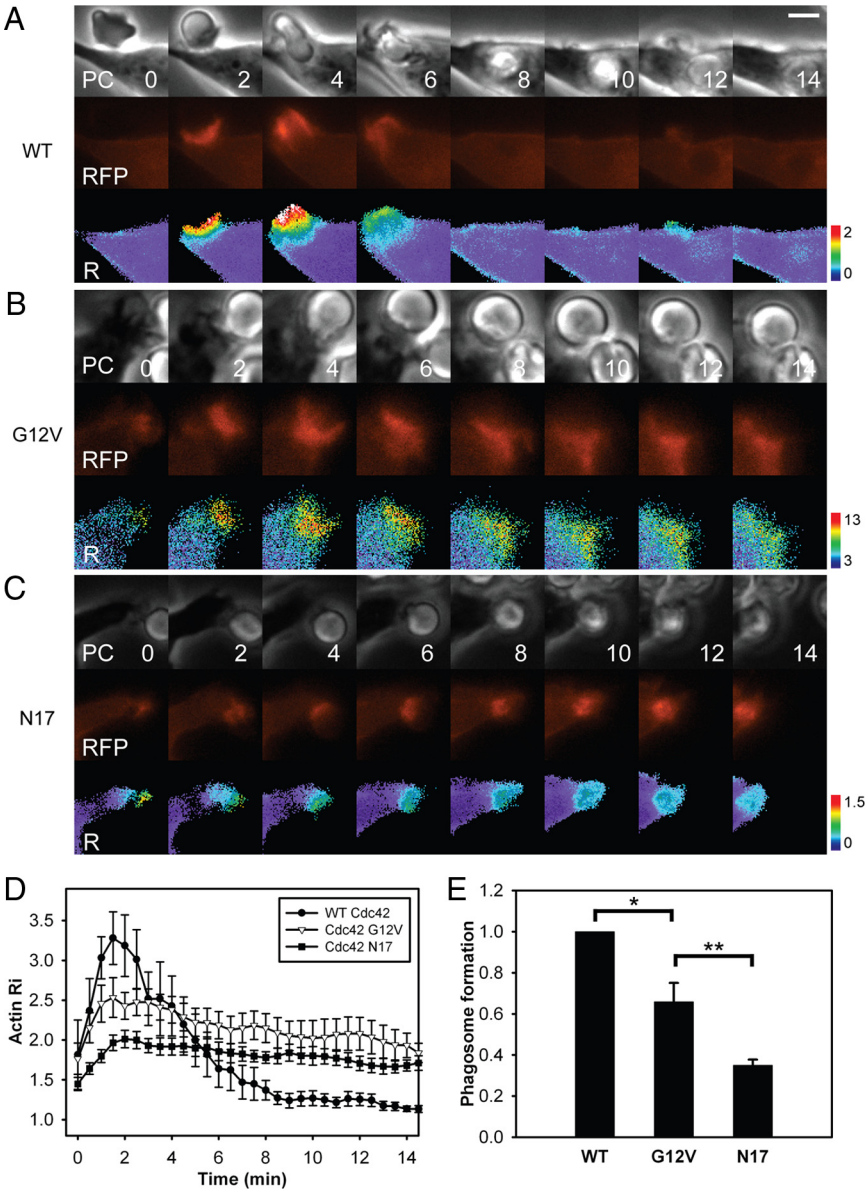

Figure 6. The Cdc42 cycle regulates actin dynamics in phagocytic cups. Images of RAW264.7 macrophages expressing mCherry-actin, CFP, and (A) YFP-Cdc42, (B) YFP-Cdc42(G12V), and (C) YFP-Cdc42(N17) during FcR-mediated phagocytosis or IgG-opsonized erythrocytes. Each series contains phase-contrast (PC), mCherry-actin (RFP), and pseudocolor Ratio (R) images (mCherry-actin/CFP ratio). Scale bar, 5 μm. Cells expressing YFP-Cdc42 were able to complete phagocytosis. (D) Recruitment of actin to forming phagosomes in cells expressing YFP-Cdc42 (●; n = 6), YFP-Cdc42(G12V) (△; n = 6), and YFP-Cdc42(N17) (■; n = 10). Time measured in minutes after erythrocyte binding to macrophage. Error bars, ±SEM. Actin dynamics evident in cells expressing WT Cdc42 were suspended by Cdc42(G12V) and Cdc42(N17) at different stages of cup formation. (E) Fraction of phagosome circumference formed during FcR-mediated phagocytosis. Cells expressing WT Cdc42 formed complete phagosomes (=1), whereas cells expressing mutant forms of Cdc42 were unable to form complete phagosomes in most cases. Error bars, ±SEM; asterisks indicate p values calculated by two-tailed *t* tests. *$p < 0.012$, **$p < 0.015$.

Cdc42(N17) rarely ingested erythrocytes. Those expressing YFP-Cdc42(G12V) formed actin-rich cups, which remained unclosed, with high concentrations of mCherry-actin at the base (Figure 6 B). Cells expressing YFP-Cdc42(N17) made only small, actin patches at points of contact with the macrophage (Figure 6C). Quantitative analysis of multiple macrophage-particle interactions revealed distinct actin dynamics for each genotypic variant of Cdc42 (Figure 6D). Cells expressing YFP-Cdc42 showed a sharp increase of actin localization at the phagosome upon particle binding, a ring-shaped band of actin that constricted the erythrocyte as it advanced over it and then decreasing levels of phagosomal actin after closure. For all Cdc42 constructs, peak actin localization occurred ~2 min after the beginning of phagocytosis. However, macrophages expressing YFP-Cdc42(G12V) and YFP-Cdc42(N17) recruited less actin to forming phagosomes relative to WT Cdc42, and both mutants showed persistent actin accumulation at the cups or points of contact. Significantly, cells expressing Cdc42(G12V) showed more actin localization to forming phagosomes than those expressing Cdc42(N17).

Further analysis of the time-lapse sequences indicated that Cdc42(G12V) allowed phagocytic cup formation to proceed further than did Cdc42(N17). For each phagocytic event, we measured the fraction of the erythrocyte enclosed by the phagocytic cup. Macrophages expressing YFP-Cdc42 formed complete phagosomes. The stalled cups formed in cells expressing YFP-Cdc42(N17) were significantly smaller than those in cells expressing YFP-Cdc42(G12V) (Figure 6E). These patterns of inhibition suggest that Cdc42 activation was required for actin polymerization that builds the cup and that subsequent deactivation of Cdc42 allows later activities required for cup closure and particle ingestion.

Thus, feedback responses linked PI3K activity and the Cdc42 activation cycle during phagocytosis. At the beginning of phagocytosis, PI3K and Cdc42 were activated following FcR ligation. Activated Cdc42 further increased PI3K activity and the accumulated 3′PIs provided a negative feed-

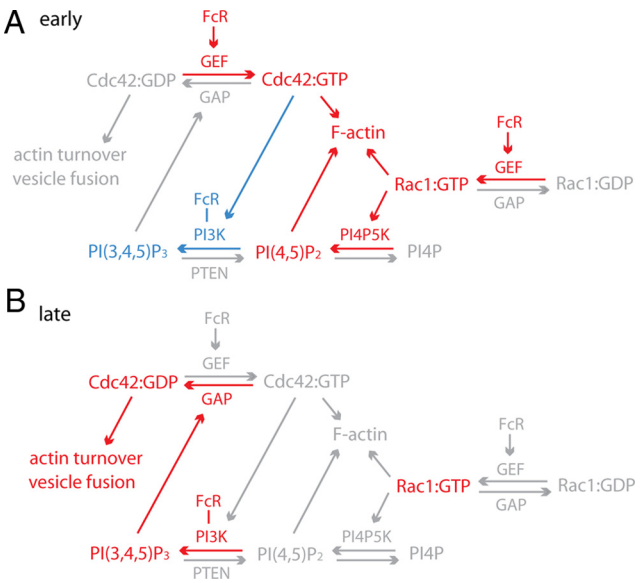

Figure 7. Summary of interactions between PI3K and Rho-family GTPases. (A) At the early stage of phagocytosis, ligated FcR mediate the activation of Cdc42, Rac1, and PI3K. Rac1:GTP and Cdc42:GTP promote the activation of PI4P5K and PI3K, respectively, which in turn generate $PI(4,5)P_2$ and $PI(3,4,5)P_3$ at phagosomes. $PI(4,5)P_2$, Rac1:GTP, and Cdc42:GTP stimulate actin polymerization, which generates force for phagocytic cup protrusion. Molecules labeled red represent high recruitment or generation around phagosomes, and molecules labeled gray represent low levels of activity. PI3K and $PI(3,4,5)P_3$ are shown in blue to indicate that they are activated at intermediate levels during early stages of phagocytosis. (B) At the late stage of phagocytosis, or the rear of the forming phagocytic cup, elevated concentrations of $PI(3,4,5)P_3$ regulate the deactivation of Cdc42, which is necessary for the closure of phagosomes. Deactivation of Cdc42 regulates actin turnover and possibly also vesicle fusion at the base of phagocytic cups.

back response to deactivate Cdc42 (Figure 7). Actin dynamics reflected the localization of Cdc42 activities.

DISCUSSION

These studies demonstrate that a PI3K-dependent signal transition of Rho-family GTPase activities occurs during FcR-mediated phagocytosis and that PI3K-dependent deactivation of Cdc42 at the signal transition is necessary for phagocytosis. Moreover, the activities of PI3K and Cdc42 are linked: FcR-activated Cdc42 stimulates PI3K, which increases concentrations of $PI(3,4,5)P_3$ in phagocytic cups, allowing the $PI(3,4,5)P_3$-dependent deactivation of Cdc42 that is necessary for completion of phagocytosis. The Cdc42 cycle regulates actin dynamics in the phagocytic cup.

Previous studies of FcR-mediated phagocytosis identified a coordinated sequence of early and late signals in forming phagocytic cups (Hoppe and Swanson, 2004; Beemiller *et al.*, 2006). Although Cdc42, Rac1, and Rac2 were persistently associated with phagosomal membranes, their patterns of activation were consistent and regular. Early signals appear at the advancing edge of the cup, some disappear a short distance from the edge (Cdc42:GTP and ARF6:GTP), and others persist throughout phagocytosis (Rac1:GTP). Late signals, which include Rac2:GTP, ARF1:GTP and PKCε (Larsen *et al.*, 2000) are delayed relative to the advancing edge of the phagosome and localize to the base of the forming cup or the fully closed phagosome. After inhibition of PI3K by LY294002, the unclosed phagocytic cups containing IgG-opsonized erythrocytes display persistently active ARF6 without activation of ARF1 (Beemiller *et al.*, 2006), which indicates that PI3K is necessary for the transition from early to late signals. The results presented here are consistent with previous studies, in that PI3K inhibition allowed sustained activation of early (Cdc42, Rac1) but not late (Rac2) signals in unclosed cups. Ratiometric imaging of YFP-CBD recruitment to phagosomes indicated that endogenous Cdc42 activities were similar to those indicated by FRET microscopy. Thus, the signal transition of Rho-family GTPase activities is also PI3K-dependent. Because TGX-221, an inhibitor specific for type I PI3Ks, generated effects similar to LY294002, we propose that $PI(3,4,5)P_3$ or $PI(3,4)P_2$ generated by type I PI3K in phagocytic cups coordinately activate the GAPs for Cdc42 and ARF6 and the GEFs for Rac2 and ARF1. It is likely that not all of these transitions are directly responsive to 3′PIs. A single 3′PI-dependent activity could regulate other changes at the signal transition. However, the additive inhibition seen in Cdc42(G12V)-expressing cells treated with LY294002 suggests that at least two PI3K-dependent activities regulate the transition.

Phagocytosis of 1–3-μm-diameter particles is relatively unaffected by PI3K inhibitors (Cox *et al.*, 1999). Three possible underlying mechanisms could explain the differential effects of PI3K inhibitors on phagocytosis of large and small particles. First, cells may employ distinct signaling pathways for phagocytosis of large and small particles. Earlier studies indicated that uptake of very small particles (immune complexes and IgG-coated microspheres $<$1-μm diameter) occurs by clathrin-dependent mechanisms (Tse *et al.*, 2003). However, the maximal size of particle for this endocytosis was smaller than the maximal size of particle for which uptake is insensitive to PI3K inhibitors. Second, PI3K-dependent activities may be present for all phagocytic activities, but only necessary to organize the construction of large phagosomes. Finally, PI3K-dependent activities may be present for all phagocytic activities but required to different extents for the construction of large and small phagosomes. We studied whether phagocytosis of large and small particles utilize different signaling pathways and found that $PI(3,4,5)P_3$ generation and Rho-family GTPase activities exhibited similar patterns of activation during phagocytosis of both 2- and 5-μm microspheres. In addition, the deactivation of Cdc42 and activation of Rac2 also require PI3K activity during phagocytosis of 2-μm microspheres. We mimicked the inhibition of GTPase deactivation by overexpressing constitutively active mutants of GTPase and found that the deactivation of Cdc42 is necessary for phagocytosis of 5-μm microspheres but less so for 2-μm microspheres. Together, these studies demonstrate that PI3K-dependent activities are present for all phagocytic activities and required to different extents for the construction of large and small phagosomes. Closure of smaller phagosomes in the presence of PI3K inhibitors may be achieved by the persisting activities of Rac1, ARF6, and Cdc42, by actin polymerization, and by PI3K-independent contractile activities (Araki *et al.*, 2003; Beemiller *et al.*, 2006).

The fact that double inhibition by Cdc42(G12V) overexpression and LY294002 treatment further reduced phagocytosis for both 2- and 5-μm microspheres also indicated that the Cdc42 activation cycle and PI3K activation are parallel signaling pathways (Figure 7). We found that constitutively active Cdc42 increased $PI(3,4,5)P_3$ in membranes of resting cells, in stalled cups around 5-μm microspheres, and during phagocytosis of 2-μm microspheres, which was consistent with a biochemical study (Zheng *et al.*, 1994). The incomplete

phagocytic cups formed on 5-μm microspheres in cells expressing YFP-Cdc42(G12V) showed less PI(3,4,5)P_3 generation than complete phagocytosis of 5-μm microspheres, indicating that maximum PI(3,4,5)P_3 generation during phagocytosis requires feedback amplification from late stage signals (Figure 7), which could include PI3K activation by FcR-associated Syk and Gab2 (Gu *et al.*, 2003). An essential feature of the signal transition was the deactivation of Cdc42, which was required to a larger extent to complete phagocytosis of larger particles.

How could the Cdc42 activation cycle organize movements for phagocytosis? Actin advances over large particles as a ring-shaped band of filaments, growing at the distal margin and disappearing at the base of the cup. Cdc42 activities show a similar ring-shaped distribution in the cup, with activation at the front, distal margin and deactivation at the back (Hoppe and Swanson, 2004). We suggest that Cdc42:GTP stimulates actin filament assembly at the distal margin of the cup, possibly through activation of WASP and Arp2/3 (Lorenzi *et al.*, 2000; May *et al.*, 2000), or by inhibition of cofilin via LIM kinase (Bierne *et al.*, 2001). PI3K-dependent deactivation of Cdc42 may facilitate actin filament turnover, which may release actin monomers for continued cup extension, allow contractile activities that shape the advancing band, or allow exocytic membrane insertion into cup membranes without interference from a cytoskeletal network (Scott *et al.*, 2005). Indeed, studies of neutrophils indicated that constitutively active Cdc42 reduces phagosome–lysosome fusion by inhibiting the depletion of actin from phagosomes (Lerm *et al.*, 2007).

Thus, the interconnected activities of PI3K and Cdc42 at the advancing edge of the phagocytic cup provide an outline of the mechanism for coordinating the different cytoskeletal activities triggered by FcR. The details of this relationship may be simple or complex. For example, the mechanism for PI3K-dependent deactivation of Cdc42 could involve a single class of protein, such as a PI(3,4,5)P_3-dependent GAP for Cdc42 or it may require a sequence of molecules, such as a PI(3,4,5)P_3-dependent GEF that activates ARF1, which in turn activates a GAP for Cdc42.

ACKNOWLEDGMENTS

We thank Dr. Samuel Straight of the Center for Live Cell Imaging at the University of Michigan for expert technical assistance. The YFP-CBD expression construct was a kind gift from Matthew F. Krummel. This work was supported by National Institutes of Health Grants AI35950 and AI64668 to J.A.S.

REFERENCES

Araki, N., Hatae, T., Furukawa, A., and Swanson, J. A. (2003). Phosphoinositide-3-kinase-independent contractile activities associated with Fcγ-receptor-mediated phagocytosis and macropinocytosis in macrophages. J. Cell Sci. *116*, 247–257.

Araki, N., Johnson, M. T., and Swanson, J. A. (1996). A role for phosphoinositide 3-kinase in the completion of macropinocytosis and phagocytosis in macrophages. J. Cell Biol. *135*, 1249–1260.

Bajno, L., Peng, X.-R., Schreiber, A. D., Moore, H.-P., Trimble, W. S., and Grinstein, S. (2000). Focal exocytosis of VAMP3-containing vesicles at sites of phagosome formation. J. Cell Biol. *149*, 697–706.

Beemiller, P., Hoppe, A. D., and Swanson, J. A. (2006). A phosphatidylinositol-3-kinase-dependent signal transition regulates ARF1 and ARF6 during Fcγ receptor-mediated phagocytosis. PLoS Biol. *4*, e162.

Bierne, H., Bouin, E., Roux, P., Caroni, P., Yin, H. L., and Cossart, P. (2001). A role for cofilin and LIM kinase in *Listeria*-induced phagocytosis. J. Cell Biol. *155*, 101–112.

Botelho, R. J., Teruel, M., Dierckman, R., Anderson, R., Wells, A., York, J. D., Meyer, T., and Grinstein, S. (2000). Localized biphasic changes in phosphatidylinositol-4,5-bisphosphate at sites of phagocytosis. J. Cell Biol. *151*, 1353–1368.

Cannon, J. L., Labno, C. M., Bosco, G., Seth, A., McGavin, M. H., Siminovitch, K. A., Rosen, M. K., and Burkhardt, J. K. (2001). Wasp recruitment to the T cell:APC contact site occurs independently of Cdc42 activation. Immunity *15*, 249–259.

Caron, E., and Hall, A. (1998). Identification of two distinct mechanisms of phagocytosis controlled by different Rho GTPases. Science *282*, 1717–1721.

Chaussade, C., *et al.* (2007). Evidence for functional redundancy of class IA PI3K isoforms in insulin signalling. Biochem. J. *404*, 449–458.

Cox, D., Chang, P., Zhang, Q., Reddy, P. G., Bokoch, G. M., and Greenberg, S. (1997). Requirements for both Rac1 and Cdc42 in membrane ruffling and phagocytosis in leukocytes. J. Exp. Med. *186*, 1487–1494.

Cox, D., Tseng, C.-C., Bjekic, G., and Greenberg, S. (1999). A requirement for phosphatidylinositol 3-kinase in pseudopod extension. J. Biol. Chem. *274*, 1240–1247.

Ge, M., Cohen, J. S., Brown, H. A., and Freed, J. H. (2001). ADP ribosylation factor 6 binding to phosphatidylinositol 4,5-bisphosphate-containing vesicles creates defects in the bilayer structure: an electron spin resonance study. Biophys. J. *81*, 994–1005.

Gu, H., Botelho, R. J., Yu, M., Grinstein, S., and Neel, B. G. (2003). Critical role for scaffolding adapter Gab2 in FcγR-mediated phagocytosis. J. Cell Biol. *161*, 1151–1161.

Henry, R. M., Hoppe, A. D., Joshi, N., and Swanson, J. A. (2004). The uniformity of phagosome maturation in macrophages. J. Cell Biol. *164*, 185–194.

Honda, A., *et al.* (1999). Phosphatidylinositol 4-phosphate 5-kinase alpha is a downstream effector of the small G protein ARF6 in membrane ruffle formation. Cell *99*, 521–532.

Hoppe, A., Christensen, K. A., and Swanson, J. A. (2002). Fluorescence resonance energy transfer-based stoichiometry in living cells. Biophys. J. *83*, 3652–3664.

Hoppe, A. D., and Swanson, J. A. (2004). Cdc42, Rac1 and Rac2 display distinct patterns of activation during phagocytosis. Mol. Biol. Cell *15*, 3509–3519.

Kavran, J. M., Klein, D. E., Lee, A., Falasca, M., Isakoff, S. J., Skolnik, E. Y., and Lemmon, M. A. (1998). Specificity and promiscuity in phosphoinositide binding by pleckstrin homology domains. J. Biol. Chem. *273*, 30497–30508.

Knapp, P. E., and Swanson, J. A. (1990). Plasticity of the tubular lysosomal compartment in macrophages. J. Cell Sci. *95*, 433–439.

Larsen, E. C., DiGennaro, J. A., Saito, N., Mehta, S., Loegering, D. J., Mazurkiewicz, J. E., and Lennartz, M. R. (2000). Differential requirement for classic and novel PKC isoforms in respiratory burst and phagocytosis in RAW 264.7 cells. J. Immunol. *165*, 2809–2817.

Lerm, M., Brodin, V. P., Ruishalme, I., Stendahl, O., and Sarndahl, E. (2007). Inactivation of Cdc42 is necessary for depolymerization of phagosomal F-Actin and subsequent phagosomal maturation. J. Immunol. *178*, 7357–7365.

Lorenzi, R., Brickell, P. M., Katz, D. R., Kinnon, C., and Thrasher, A. J. (2000). Wiskott-Aldrich syndrome protein is necessary for efficient IgG-mediated phagocytosis. Blood *95*, 2943–2946.

Manser, E., Leung, T., Salihuddin, H., Tan, L., and Lim, L. (1993). A non-receptor tyrosine kinase that inhibits the GTPase activity of p21cdc42. Nature *363*, 364–367.

Marshall, J. G., Booth, J. W., Stambolic, V., Mak, T., Balla, T., Schreiber, A. D., Meyer, T., and Grinstein, S. (2001). Restricted accumulation of phosphatidylinositol 3-kinase products in a plasmalemmal subdomain during Fc gamma receptor-mediated phagocytosis. J. Cell Biol. *153*, 1369–1380.

May, R. C., Caron, E., Hall, A., and Machesky, L. M. (2000). Involvement of the Arp2/3 complex in phagocytosis mediated by FcγR and CR3. Nat. Cell Biol. *2*, 246–248.

Melendez, A. J., Harnett, M. M., and Allen, J. M. (2001). Crosstalk between ARF6 and protein kinase C_α in FcγRI-mediated activation of phospholipase D1. Curr. Biol. *11*, 869–874.

Niedergang, F., Colucci-Guyon, E., Dubois, T., Raposo, G., and Chavrier, P. (2003). ADP ribosylation factor 6 is activated and controls membrane delivery during phagocytosis in macrophages. J. Cell Biol. *161*, 1143–1150.

O'Luanaigh, N., Pardo, R., Fensome, A., Allen-Baume, V., Jones, D., Holt, M. R., and Cockcroft, S. (2002). Continual production of phosphatidic acid by phospholipase D is essential for antigen-stimulated membrane ruffling in cultured mast cells. Mol. Biol. Cell *13*, 3730–3746.

Scott, C. C., Dobson, W., Botelho, R. J., Coady-Osberg, N., Chavrier, P., Knecht, D. A., Heath, C., Stahl, P., and Grinstein, S. (2005). Phosphatidylino-

sitol-4,5-bisphosphate hydrolysis directs actin remodeling during phagocytosis. J. Cell Biol. *169*, 139–149.

Srinivasan, S., Wang, F., Glavas, S., Ott, A., Hofmann, F., Aktories, K., Kalman, D., and Bourne, H. R. (2003). Rac and Cdc42 play distinct roles in regulating PI(3,4,5)P_3 and polarity during neutrophil chemotaxis. J. Cell Biol. *160*, 375–385.

Swanson, J. A. (2008). Shaping cups into phagosomes and macropinosomes. Nat. Rev. Mol. Cell Biol. *9*, 639–649.

Swanson, J. A., Johnson, M. T., Beningo, K., Post, P., Mooseker, M., and Araki, N. (1999). A contractile activity that closes phagosomes in macrophages. J. Cell Sci. *112*, 307–316.

Tse, S.M.L., Furuya, W., Gold, E., Schreiber, A. D., Sandvig, K., Inman, R. D., and Grinstein, S. (2003). Differential role of actin, clathrin, and dynamin in Fcγ receptor-mediated endocytosis and phagocytosis. J. Biol. Chem. *278*, 3331–3338.

Tskvitaria-Fuller, I., Seth, A., Mistry, N., Gu, H., Rosen, M. K., and Wulfing, C. (2006). Specific patterns of Cdc42 activity are related to distinct elements of T cell polarization. J Immunol. *177*, 1708–1720.

Usui, I., Imamura, T., Huang, J., Satoh, H., and Olefsky, J. M. (2003). Cdc42 is a Rho GTPase family member that can mediate insulin signaling to glucose transport in 3T3-L1 adipocytes. J. Biol. Chem. *278*, 13765–13774.

Vieira, O. V., Botelho, R. J., Rameh, L., Brachmann, S. M., Matsuo, T., Davidson, H. W., Schreiber, A., Backer, J. M., Cantley, L. C., and Grinstein, S. (2001). Distinct roles of class I and class III phosphatidylinositol 3-kinases in phagosome formation and maturation. J. Cell Biol. *155*, 19–25.

Zhang, Q., Cox, D., Tseng, C.-C., Donaldson, J. G., and Greenberg, S. (1998). A requirement for ARF6 in Fcγ receptor-mediated phagocytosis in macrophages. J. Biol. Chem. *273*, 19977–19981.

Zheng, Y., Bagrodia, S., and Cerione, R. A. (1994). Activation of phosphoinositide 3-kinase activity by Cdc42Hs binding to p85. J. Biol. Chem. *269*, 18727–18730.